Article

Not peer-reviewed version

# Contactless Detection of pH Change in a Liquid Analyte

Dylan Gustafson * and Dominic Klyve

Posted Date: 14 March 2025

doi: 10.20944/preprints202503.0963.v1

Keywords: sensor; pH; radiofrequency; contactless; microwave; non-invasive

 doi:10.20944/preprints202503.0963.v1



*Article*

# Contactless Detection of pH Change in a Liquid Analyte

**Dylan Gustafson [1,*] and Dominic Klyve [2]**

[1] Department of Mathematics, Central Washington University, Ellensburg 98926, USA
[2] Know Labs, Inc.
* Correspondence: dylan.gustafson@cwu.edu

**Abstract:** We describe an experiment in which we employ a radiofrequency sensor to measure pH changes in a liquid solution. The experiment is novel in a few ways. First, the sensor does not have contact with the liquid, but rather detects the change from the outside of a PVC pipe. Second, the change is detected using a Linear Discriminant Analysis model using values from an inverse Fourier transform of the frequency data as its features. We believe this to be the first use of Fourier anaylsis in contactless pH measurement using radio frequencies.

**Keywords:** sensor; pH; radiofrequency; contactless; microwave; non-invasive

## 1. Introduction

Accurate and reliable measurement of pH levels is vital across a broad range of applications, including industrial processes [1], agricultural [2] and environmental monitoring [3,4], and biomedical diagnostics [5,6]. Conventional methods, such as optical and electrode-based pH meters, are widely used due to their demonstrated accuracy and ease of use. However, these methods have limitations, primarily stemming from the need for direct contact with the analyte.

Microwave and radio frequency (RF)-based sensing have recently emerged as promising alternatives for non-invasive chemical analysis [7,8]. Unlike conventional approaches, RF-based sensors can offer rapid, contactless measurements, making them particularly suited for industrial applications where a shutdown required to repair or make changes to inline sensors would be too costly, or where the analyte itself is too corrosive to put in direct contact with a sensor. Some earlier work has shown that RF may be a promising tool for the detection of pH. One previous study demonstrated that pH can be measured using RF combined with chemical exchange saturation transfer (CEST) Magnetic Resonance Imaging (MRI) techniques [7]. While promising, this technique has the obvious limitation of requiring MRI hardware. Other work has attempted to differentiate between five standard pH buffer solutions by placing the solution directly on an RF planar microstrip antenna [8]. While promising, this work is limited by the use of a single resonant frequency in the analysis, and by the fact that these five standard solutions are chemically different in ways other than their pH value.

RF-based pH sensors face significant challenges. Chief among these are its inability to pass through metal, the sensitivity required to measure minuscule changes in hydronium concentration, and the ability to measure pH consistently regardless of acid type or other substances present in solution. Just as traditional electrode-based pH meters are incompatible with particular substances such as organic solvents, hot caustics, soiling media, or abrasives [1] depending on their specific design, certain substances in a solution may obscure or overwhelm RF-based pH measurements, rendering them incompatible for a pH sensor of this kind. Addressing these challenges is crucial to advancing RF sensing technologies and expanding their applicability to real-world scenarios.

This study presents a novel approach to pH detection using a microwave-based sensor system that captures frequency response curves across a range of pH values. By applying discrete Fourier transform (DFT) analysis, we identify sinusoidal patterns in the frequency response data that correspond strongly with pH levels. These patterns enable the development of a simple yet robust algorithm for categorizing

 doi:10.20944/preprints202503.0963.v1



pH values, achieving high accuracy in our experimental tests over selected pH ranges. We believe this to be the first use of a DFT to analyze pH changes using RF spectroscopy.

## 2. Materials and Methods

The sensor employed in this study is the patented Know Labs, Inc., RF dielectric sensor, which consists of a printed circuit board assembly (PCBA) that generates RF signals and measures received power after passing those signals through an antenna array on a separate PCBA. The device measures the total received RF power at port 2 while transmitting a frequency sweep from port 1, which is a proxy for the forward transmission coefficient of the system, $S_{21}$. See [9] for a detailed description of the sensor assembly.

The analyte solution is contained in a 3-inch PVC pipe end cap (Part# 3P06 from NDS Inc.), meant to mimic a cross-section of plastic pipe. This has a capacity of around 200ml. The PCBA containing the sensor's antenna array is held in place against the round wall of the PVC cap using a custom 3D-printed fixture, and is connected to the RF-generating PCBA via SMP cables. This RF-generating PCBA is controlled by a computer connected via USB. All components are taped down to the work surface to prevent them from moving during an experiment, however the position of the antenna relative to the analyte is maintained much more precisely by fasteners and press-fit hardware. This hardware can be seen in Figure 1.

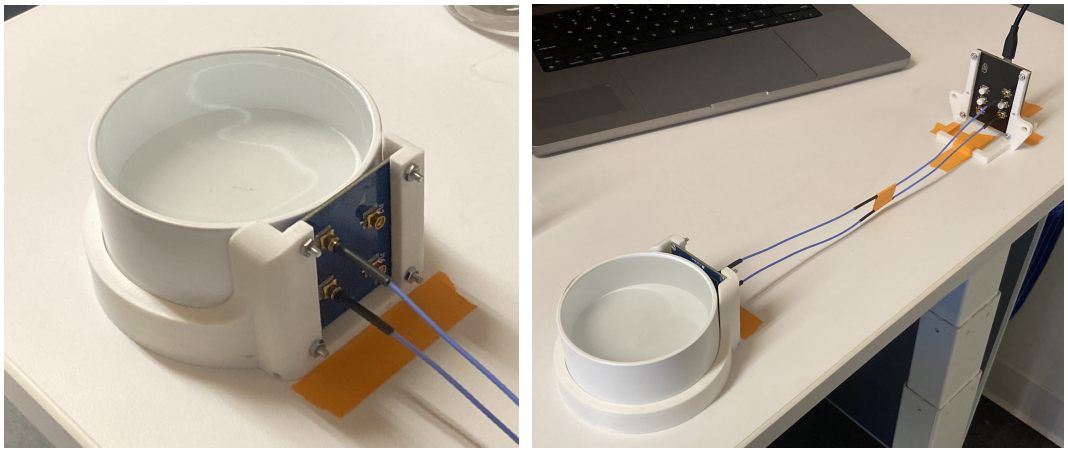

(**a**) (**b**)

**Figure 1.** Experimental setup: **(a)** Antenna board positioned against the PVC vessel. **(b)** Connection via SMP cables to separate RF-generating board.

Kroger-brand distilled water was used as the baseline analyte. Due to its absorption of carbon dioxide from the air and lack of dissolved minerals to provide buffering, this water has a pH around 5.5. During the experiment, the pH was lowered to a final "target" value by replacing some volume of the water with an equivalent volume of either 1 molar (M) sulfuric acid ($H_2SO_4$) or 1M hydrochloric acid (HCl). For this initial study, the scope was limited to pH target values 1, 2, 3, 4, and 5. This meant that all final pH values could be achieved by adding acid to distilled water, as all of these target values are below 5.5. Whole numbers were chosen simply out of convenience.

The procedure for each test run is as follows:

1. Rinse out the PVC cap with distilled water and dry with a lint-free towel.
2. Install the PVC cap and antenna board into the fixture.
3. Measure out 200.0g of distilled water on an AWS scale; part number AWS-600-BLK.
4. Transfer the water into the cap, and allow it to settle for at least 20 seconds. Begin running microwave sweeps from 300MHz to 4100MHz at frequency intervals of 5MHz.
5. This first "baseline" run performs 300 - 4100 MHz sweeps for 120 seconds, generating 47 rows of data, before pausing.

 doi:10.20944/preprints202503.0963.v1



6. Once paused, remove the determined replacement volume of water using a micropipette.
7. Add the same replacement volume of acid solution to the cap vessel using a micropipette.
8. Mix in the acid using back-and-forth stirring motions to avoid creating a lasting vortex. Take care not to move any component of the test fixture; avoid bumping the walls of the cap vessel with the stirring stick.
9. After stirring, wait at least another 30 seconds and then restart the sweeps.
10. This final "change" run performs 300 MHz - 4100 MHz sweeps for another 120 seconds, generating another 47 rows of data.
11. Once the sweeps are complete and the script exits, dump the solution and rinse out the vessel with distilled water.

This procedure was performed with both HCl and $H_2SO_4$, targeting final pH values 1, 2, 3, 4, and 5, for a total of 10 different experiment types. Each experiment type was repeated 10 times, (with the exception of the pH 1 HCl test, which was only performed 5 times), yielding a total of 95 runs of this procedure. For testing 200ml of solution at a time, the acid replacement volumes needed to achieve each target pH value is given in Table 1. The $H_2SO_4$ replacement volumes were calculated using weak acid equilibrium calculations, assuming a pKa of 1.988 for bisulfate.

**Table 1.** Volumes of water replaced with 1M acid solution to create the desired final pH in the 200ml vessel.

| Final pH | 1M $H_2SO_4$ Volume (µL) | 1M HCl Volume (µL) |
|---|---|---|
| 1 | 18,300 | 20,000 |
| 2 | 1,300 | 2,000 |
| 3 | 104 | 200 |
| 4 | 10 | 20 |
| 5 | 1 | 2 |

Additionally, 10 runs of a "mock" change experiment were performed, for a grand total of 105 experiments. This mock experiment followed the same procedure as above, except none of the distilled water was replaced. During the pause between the two 47-sweep runs, the water was merely stirred in the same fashion.

## 3. Results

The device records each sweep result as a vector of voltage values. Each value represents the voltage measured in the receiving antenna when the transmitting antenna was generating a specific frequency. Since each sweep covers the frequency range 300 MHz to 4100 MHz, stepping upwards by 5 MHz, each sweep will generate 760 voltage measurements. Plotting this data with voltage (V) on the vertical axis and frequency (MHz) on the horizontal axis creates a "frequency response curve". Each of the 105 total experiments generated two sets of 47 frequency response curves to consider: "baseline" response curves for the distilled water and "final" response curves for the acidic solution.

Each experiment was first analyzed for signal drift by looking at the voltage values across its 47 "baseline" sweeps and 47 "final" sweeps. In "baseline" series, the mean voltage values among the first 20 sweeps was compared to that of the remaining 27 sweeps. No statistically significant drift was found, which helped rule out the potential for false positives in a real-time measurement environment. Experiments were then summarized by taking the mean "final" curve minus the mean "baseline" curve, creating a mean "change" curve for each experiment. The mean "change" curves from the "mock" change experiments were used as a control against which to judge the "change" curves from the "real" experiments. Any feature that appeared in both the "real" change curves and the "mock" change curves was ignored.

When plotting the change curves, as seen in Figure 2, one can see that those corresponding to pH values 1, 2, and 3 are nearly sinusoidal in the 1140 MHz – 1890 MHz domain. These "sine waves" all have a wavelength of around 185 MHz, and are in roughly the same phase, while their amplitudes

 doi:10.20944/preprints202503.0963.v1



increase with lower pH values (higher hydronium concentration). Interestingly, the amplitudes for the pH 2 HCl tests roughly match that of pH 2 $H_2SO_4$ tests. Similarly, the pH 3 HCl amplitudes roughly match those of the pH 3 $H_2SO_4$ solutions. This is true for the pH 1 tests to some extent, although these response curves were noisier. All of this supports the idea that the sinusoidal shapes in the "change" curves are caused specifically by the hydronium ions in the solution, as opposed to the chloride or sulfate anions. This distinction is crucial for true pH measurement.

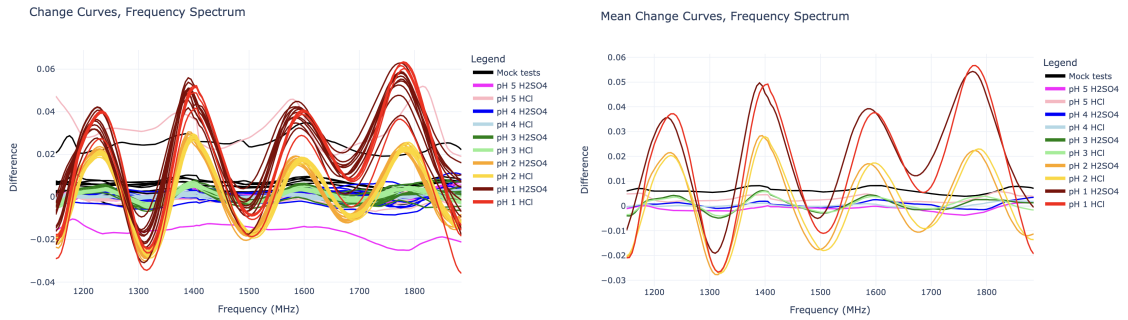


(**a**) (**b**)

**Figure 2.** Energetic response vs frequency plots ("change curves") in the 1140 MHz – 1890MHz domain: **(a)** All experiment curves plotted individually. **(b)** Mean curves for each experiment type.

The goal with this data is to train a machine learning model to predict pH from RF data. Accordingly, these 105 change curves were divided into a "training" set to train the model, and a "test" set to evaluate its performance. With 10 runs for each experiment type, the first 5 were placed in the training set, while the remaining 5 were placed in the test set. However, since the pH 1 HCl experiments had only had 5 runs in total, the first 2 of these runs went to the "training" set while the remaining 3 went to the "test" set, resulting in a total of 52 "training" experiments and 53 "test" experiments. Figure 3 shows change curve plots of all 52 experiments in the "training" set. Since the goal is to detect any change in pH, the prediction algorithm must make no distinction based on acid type. Thus, the Figure 3 plots are grouped by pH only.

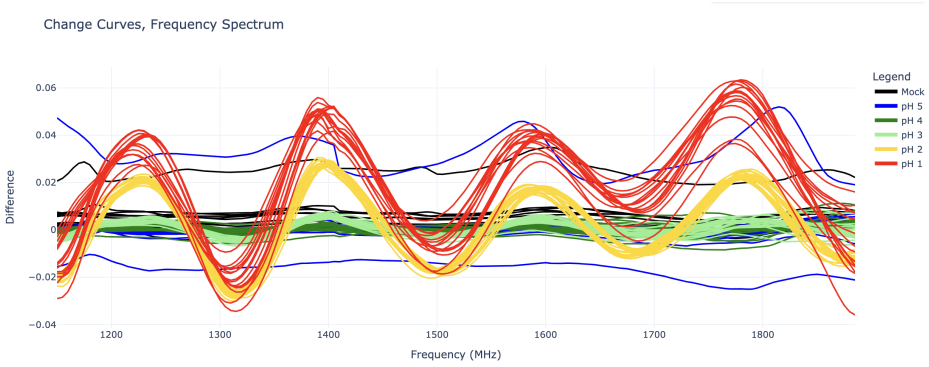


**Figure 3.** Change curves for all experiments in the "training" set.

Due to the clear sinusoidal patterns over the 1140 MHz – 1890 MHz domain, each change curve was truncated to this domain and fed into an inverse discrete Fourier transform (IDFT) for deeper analysis. (Note: Functionally there is little difference between forward and inverse Fourier transforms, however because the change curves were already a frequency spectrum, an inverse transform seemed more appropriate.) Because the sinusoidal curves exhibit four periods along the given domain, the inverse discrete Fourier transform of these curves show clear impulses at coefficient 4. The magnitude of IDFT coefficients 0 through 7 for each experiment can be seen in Figure 4.

 doi:10.20944/preprints202503.0963.v1



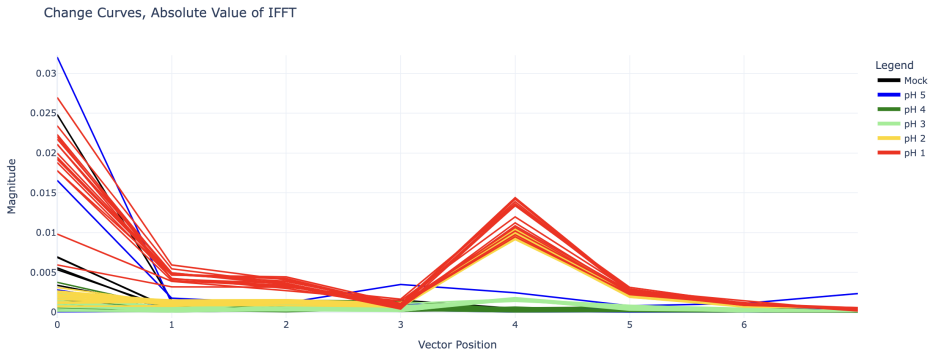


**Figure 4.** The first 8 inverse discrete Fourier transform (IDFT) coefficient magnitudes for all experiments in the "training" set.

If the plots in Figure 3 depicted a true frequency domain plot of the signal received by the antenna, these inverse Fourier transforms would imply the antenna experienced a delayed voltage impulse. However, the Figure 3 plots actually depict a measure of the total energy received by the Rx antenna when the Tx antenna was transmitting a wave at the given frequency. These energy values are measured one-at-a-time for each frequency, and thus does not represent the Fourier transform of a single time-domain signal.

The value of these IDFT coefficients can be used to predict the pH of the analyte. There is high selectivity between the coefficient 4 values for pH 2, pH 3, and pH 4 (for which coefficient 4 is nearly zero). The pH 1 curves also show some difference in coefficient 4, but this is not as clear. However, because the pH 1 curves in Figure 3 appear to be shifted upwards as well, especially in the right half (1500 – 1890 MHz), their inverse Fourier transforms all have large values in coefficients 0, 1, and 2 as well.

On the other hand, the change curves for pH 4 and pH 5 cannot be easily distinguished from "mock" change curves, as they do not show any sinusoidal behavior or consistent vertical shifts. The pH 5 tests in particular are also quite misbehaved, as they contain some outliers with large vertical shifts, as seen in Figure 5.

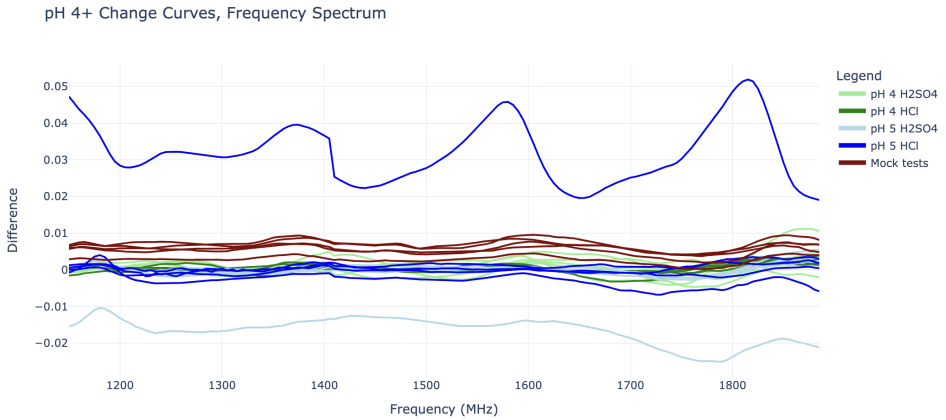


**Figure 5.** Change curves for all pH 4, pH 5, and "mock" experiments from the "training" set. Plot in frequency domain along 1140 MHz – 1890 MHz.

The most severe pH 5 outlier, visible as the highest blue line in Figure 5, is suspected to have been caused by a connection issue with the SMP cables. The curve's periodic shape is actually significant enough to give it a substantial coefficient 4 value in its IDFT, placing it between that of the pH 2 and pH 3 curves (this can be seen in Figure 4). However, it can still be distinguished from all pH 2 and pH 3 curves by its substantial vertical shift, represented by its IDFT coefficient 0.

 doi:10.20944/preprints202503.0963.v1



### 3.1. Detection Algorithm

These results were used to build a pH change detection algorithm that could theoretically be used to detect pH changes in real time. For this limited-scope project, it was decided to use a classification method rather than a regression method, meaning that the detection algorithm would read in data and predict either "No change" or an integer pH value from 1 to 5, rather than attempting to calculate a continuous pH value.

It is clear that distinguishing pH values 1, 2, and 3 from pH values 4 or higher is easier than separating pH 4, pH 5, and "No change". Thus, it was decided to split the detection algorithm into two stages. The first stage would use a pretrained model to classify the an experiment as pH 1, pH 2, pH 3, or "pH 4+", then a separate pretrained model would classify the "pH 4+" experiments as pH 4, pH 5, or "No change". The 52 experiments from the "training" set were used to train each model, while the remaining 53 experiments were fed into the final algorithm to evaluate its accuracy.

As seen in Figure 3, it takes a combination of Fourier coefficients to fully distinguish each pH value, thus pH classification can be predicted from these coefficients using a Linear Discriminant Analysis (LDA) model. The specific software employed was the LinearDiscriminantAnalysis package from scikit-learn version 1.6.1 [10] in Python 3.11. While it is likely that other models (PCA, wavelet transforms) would have had similar results, the visual separation in the signal among the various pH solutions suggested that a simple model would be best.

In the first stage, the magnitude of Fourier coefficients 0 and 4 were used to train a 2-dimensional LDA classifier with the categories "pH 1", "pH 2", "pH 3", and "pH 4+". After training the classifier on the entire "training" set, it was able to predict all of the pH classifications in the "test" set with 100% accuracy. The decision boundaries along with the "training" and "test" data can be seen in Figure 6, while the confusion matrix for this classifier can be seen in Figure 7.

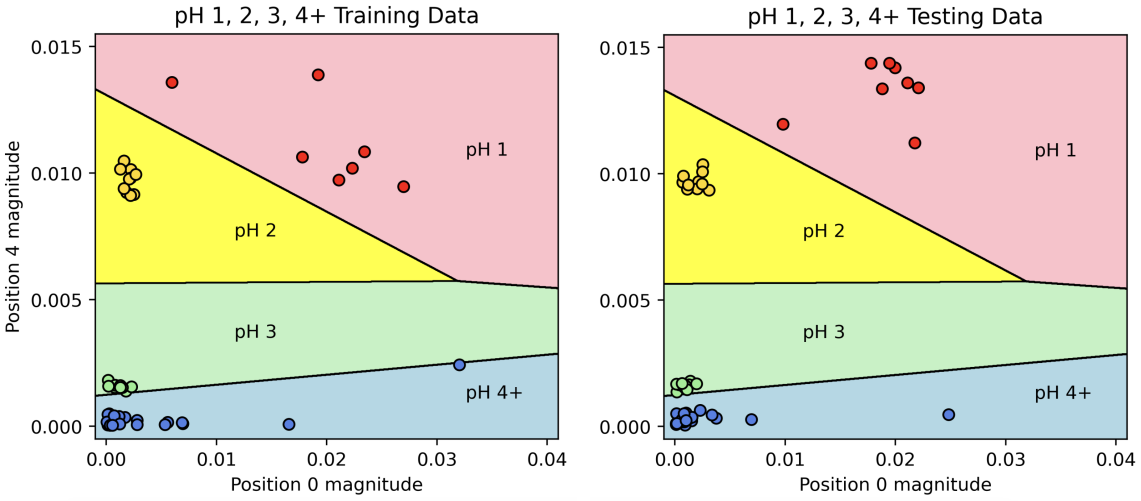


**Figure 6.** Scatter plots of IDFT vector position 0 and 4 values for **(a)** "training" data and **(b)** "test" data, along with the LDA model's decision boundaries.

Preprints.org (www.preprints.org) | NOT PEER-REVIEWED | Posted: 14 March 2025 doi:10.20944/preprints202503.0963.v1



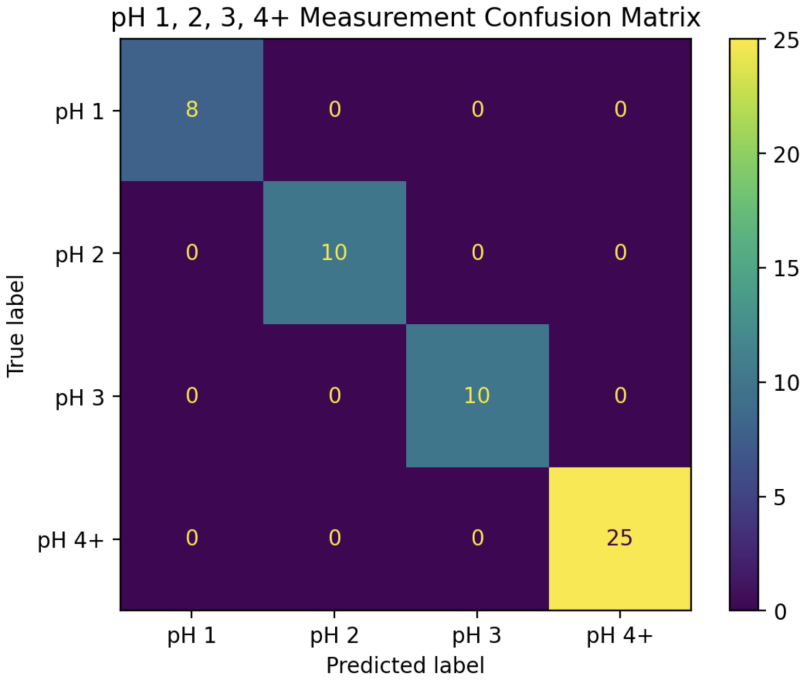


**Figure 7.** Confusion matrix for the pH 1, 2, 3, and 4+ LDA classifier applied to the "test" set, indicating its 100% accuracy.

The second classifier was designed to deal only with pH 4+ experiments, attempting to further classify them as either pH 4, pH 5, or "No change". To guard against data leakage, the same training and test sets described above were used for this second phase. As seen in Figure 5, these three categories are much more difficult to distinguish, however there is still some noticeable variability. In particular, plotting the real parts of the IDFT coefficients rather than their magnitudes revealed some potential separability. Scatter plots comparing the real parts of coefficients 0, 1, and 2 are shown in Figure 8.

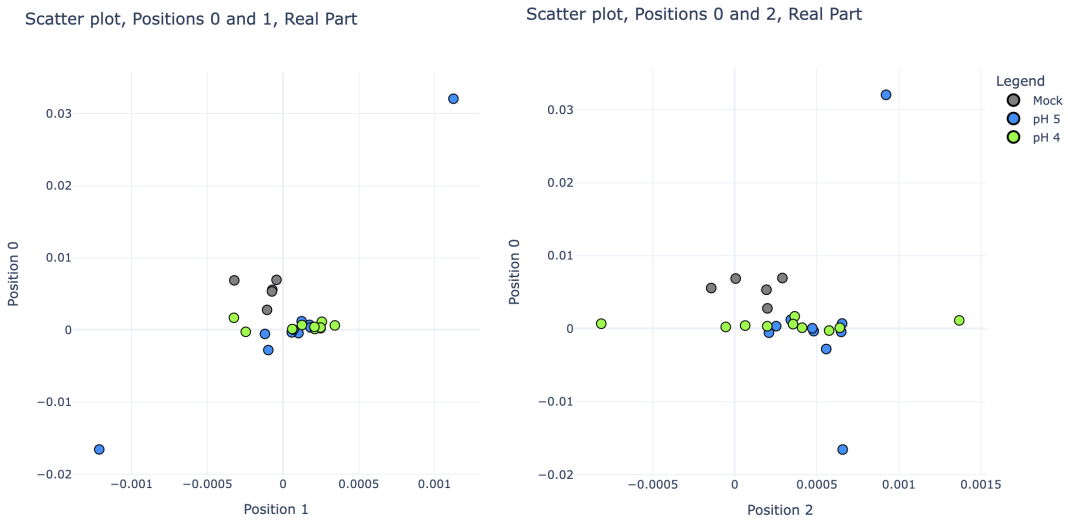


(**a**) (**b**)

**Figure 8.** Scatter plots comparing the real parts of IDFT coefficients For pH 4, pH 5, and "mock" experiments (training set only). **(a)** Coefficients in position 0 vs position 1. **(b)** Coefficients in position 0 vs position 2.

A new LDA model was trained using the real parts of the IDFT coefficients for pH 4, pH 5, and "mock" experiments from the training set. To maximize the performance and efficiency of this model,

 doi:10.20944/preprints202503.0963.v1



stepwise regression was employed by starting with IDFT coefficient 0 alone, then adding subsequent coefficients into the model one at a time while tracking its resulting prediction accuracy on the "test" series. After the inclusion of coefficient 4, no further improvements to the model could be made. Thus, the "second phase" of the pH detection algorithm became a 5-Dimensional LDA classifier, using the real parts of IDFT coefficients 0, 1, 2, 3, and 4. The confusion matrix in Figure 9 shows the performance when using this model to classify all of the pH 4+ experiments from the "test" set into pH 4, pH 5, and "No change".

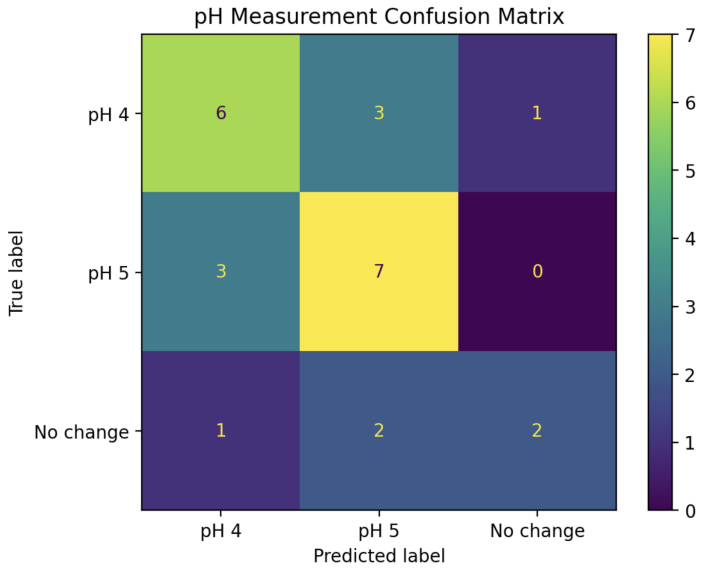


**Figure 9.** Confusion matrix for the pH 4, pH 5, and "No change" LDA classifier applied to all pH 4+ experiments from the "test" set, which by itself achieves only 60% accuracy.

Putting these two LDA classifiers together creates a two-step pH prediction algorithm. For a given change curve, the magnitude of IDFT coefficients 0 and 4 are first fed into the 2-dimensional LDA model to classify it as pH 1, 2, 3, or 4+. For those classified as pH 4+, the real parts of coefficients 0 through 4 are then fed into the 5-dimensional LDA model to further classify it as pH 4, pH 5, or "No change". The confusion matrix for this complete algorithm applied to all 53 experiments in the "test" set is shown in Figure 10.

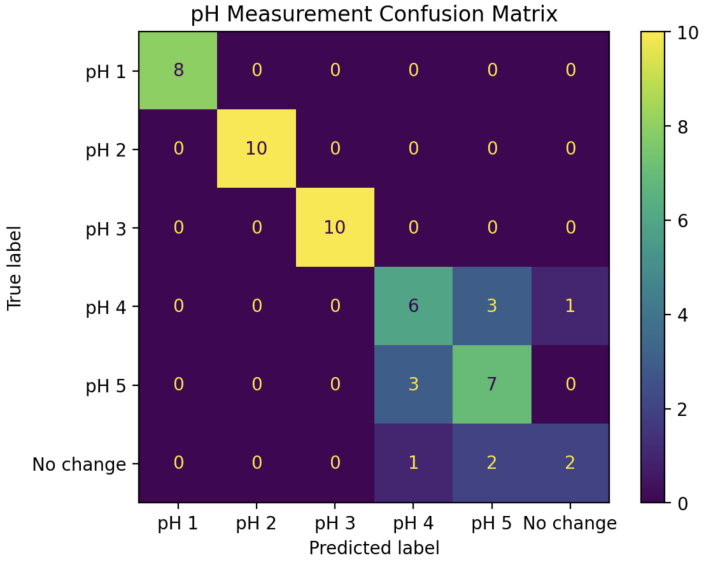


**Figure 10.** Confusion matrix for pH predictions of all 53 experiments in the "test" set.

 doi:10.20944/preprints202503.0963.v1



This combined algorithm has a prediction accuracy of 81%, including 100% accuracy for pH values 1, 2, and 3.

## 4. Discussion

These results demonstrate the power of combining a sensor employing RF spectroscopy and analysis using a discrete Fourier transform to detect and measure pH changes caused by small changes to a liquid solution. The use of Fourier analysis was a particularly novel feature in this work. While previous studies have demonstrated the sensor's ability to detect changes in blood glucose levels [9,11,12], the data processing for these studies was performed on the raw values received by the sensor. This suggests interesting analysis possibilities in related studies using Fourier transforms in the future.

When solutions were split into four categories (pH 1, 2, 3, or 4+), an LDA model trained using the Fourier coefficients achieved 100% prediction accuracy. When pH 5 was included as its own category, the model was less successful. This is unsurprising, as a change from pH 5.5 to pH 5 is quite small. Even these results were encouraging, however – 70% of pH 5 solutions were identified as being pH 5, and the remaining 30% were classified as pH 4 as opposed to "No change". Indeed, across the 48 experiments in the "test" set where pH was changed, the model successfully detected change in 47 of these, giving a positive predictive rate of 98% for pH change detection of any kind. Equally interesting is the simplicity of the final model; while many Fourier coefficients were available to the model, the predictive accuracy for the pH 1, 2, 3, and 4+ classifier was achieved using a rather simple two-dimensional LDA model, allowing for 2D graphs such as the one shown in Figure 6.

The experiment series used for this analysis is limited in scope. For example, all experiments started with pure water and ended at a lower pH. There were no experiments that involved first lowering the pH, then raising it again to confirm the response curve returns to its original position, or vice versa. Thus, it is possible that the measurements are more indicative of the solution's electrical conductivity than its pH, and future work will attempt to distinguish these types of measurements.

Despite the limitations, this project is a promising start, as even very small changes to the liquid solution were detected by the algorithm with 100% accuracy. To achieve pH 3, only 104 µL water out of 200mL total was replaced with 1M $H_2SO_4$ (or 200 µL in the case of 1M HCl). This indicates the sensor's high level of sensitivity, and it is reasonable to assume this sensor could detect many other types of small changes. Future work will explore some of these possibilities as well.

**Author Contributions:** Test apparatus design, experiment conduction, data collection, creation of prediction model and figures, and much of the article writing was performed by Dylan Gustafson. Project management, technical oversight, additional data analysis, and additional article writing performed by Dominic Klyve. Conceptualization, D.G. and D.K.; methodology, D.G. and D.K.; software, D.G. and D.K.; validation, D.G.; formal analysis, D.G. and D.K; investigation, D.G.; resources, D.G.; data curation, D.G.; writing—original draft preparation, D.G.; writing—review and editing, D.G. and D.K.; visualization, D.G.; supervision, D.K.; project administration, D.K.; funding acquisition, D.K. All authors have read and agreed to the published version of the manuscript.

**Funding:** This research was funded entirely by Know Labs, Inc.

**Data Availability Statement:** Dataset available on request from the authors.

**Acknowledgments:** Mahi Karim, Patrick Kasl, and Barry Shelton for reviewing.

**Conflicts of Interest:** DG is a consultant for Know Labs. DK is employed by and owns stock in Know Labs.

## Abbreviations

The following abbreviations are used in this manuscript:

| | |
|---|---|
| RF | Radio frequency |
| MRI | Magnetic resonance imaging |
| DFT | Discrete Fourier transform |

 doi:10.20944/preprints202503.0963.v1



| | |
|---|---|
| IDFT | Inverse discrete Fourier transform |
| PCBA | Populated circuit board assembly |
| SMP | Sub-miniature push-on |
| PVC | Polyvinyl chloride |
| HCl | Hydrochloric acid |
| $H_2SO_4$ | Sulfuric acid |
| LDA | Linear discriminant analysis |

## References


1. Endress+Hauser, "pH measurement in industrial processes." [Online] pp. 22–36. Available: https://portal.endress.com/dla/5000455/3062/000/01/CP00010C24EN1315_US%20ph%20sel%20guide.pdf
2. G. B. Penner, K. A. Beauchemin, and T. Mutsvangwa, "An Evaluation of the Accuracy and Precision of a Stand-Alone Submersible Continuous Ruminal pH Measurement System," *J. Dairy Sci.*, vol. 89, no. 6, pp. 2132–2140, Jun. 2006, doi: 10.3168/jds.S0022-0302(06)72284-6.
3. B. M. Saalidong, S. A. Aram, S. Otu, and P. O. Lartey, "Examining the dynamics of the relationship between water pH and other water quality parameters in ground and surface water systems," *PLOS ONE*, vol. 17, no. 1, e0262117, Jan. 2022, doi: 10.1371/journal.pone.0262117.
4. S. Viciano-Tudela, L. Parra, S. Sendra, and J. Lloret, "A Low-Cost Virtual Sensor for Underwater pH Monitoring in Coastal Waters," *Chemosensors*, vol. 11, no. 4, Art. no. 4, Apr. 2023, doi: 10.3390/chemosensors11040215.
5. L. Guo *et al.*, "Portable Photoacoustic Analytical System Combined with Wearable Hydrogel Patch for pH Monitoring in Chronic Wounds," *Anal. Chem.*, vol. 96, no. 28, pp. 11595–11602, Jul. 2024, doi: 10.1021/acs.analchem.4c02472.
6. A. Balla *et al.*, "Manometric and pH-monitoring changes after laparoscopic sleeve gastrectomy: a systematic review," *Langenbecks Arch. Surg.*, vol. 406, no. 8, pp. 2591–2609, Dec. 2021, doi: 10.1007/s00423-021-02171-3.
7. R. Wu, D. L. Longo, S. Aime, and P. Z. Sun, "Quantitative description of radiofrequency (RF) power-based ratiometric chemical exchange saturation transfer (CEST) pH imaging," *NMR Biomed.*, vol. 28, no. 5, pp. 555–565, 2015, doi: 10.1002/nbm.3284.
8. A. Bouchalkha and R. Karli, "Planar Microstrip Antenna Sensor for pH Measurements," in *2019 International Conference on Electrical and Computing Technologies and Applications (ICECTA)*, Nov. 2019, pp. 1–5. doi: 10.1109/ICECTA48151.2019.8959701.
9. D. Klyve, S. Lowe, K. Currie, J. H. Anderson, C. Ward, and B. Shelton, "Non-Invasive Blood Glucose Measurement Using RF Spectroscopy and a lightGBM AI Model," *IEEE Sens. J.*, pp. 28049–28055, 2024, doi: 10.1109/JSEN.2024.3405800.
10. F. Pedregosa *et al.*, "Scikit-learn: Machine Learning in Python," *J. Mach. Learn. Res.*, vol. 12, no. 85, pp. 2825–2830, 2011.
11. D. Klyve, J. H. Anderson, G. Lorentz, and V. K. Somers, "Detecting Unique Analyte-Specific Radio Frequency Spectral Responses in Liquid Solutions—Implications for Non-Invasive Physiologic Monitoring," *Sensors*, vol. 23, no. 10, Art. no. 10, Jan. 2023, doi: 10.3390/s23104817.
12. F. Karim, J. H. Anderson, K. Currie, C. Bui, D. Klyve, and V. K. Somers, "A Glycemic Status Classification Model Using a Radiofrequency Noninvasive Blood Glucose Monitor," *Diabetes Technol. Ther.*, vol. 26, no. 12, pp. 979–983, Dec. 2024, doi: 10.1089/dia.2024.0170.